Peristaltic Transport of a Hyperbolic Tangent Fluid Model in an Asymmetric Channel

Sohail Nadeem and Safia Akram

Department of Mathematics, Quaid-i-Azam University 45320, Islamabad 44000, Pakistan

Reprint requests to S. N; E-mail: snqau@hotmail.com

Z. Naturforsch. **64a,** 559 – 567 (2009); received August 18, 2008 / revised December 4, 2008

In the present analysis, we have modeled the governing equations of a two dimensional hyperbolic tangent fluid model. Using the assumption of long wavelength and low Reynolds number, the governing equations of hyperbolic tangent fluid for an asymmetric channel have been solved using the regular perturbation method. The expression for pressure rise has been calculated using numerical integrations. At the end, various physical parameters have been shown pictorially. It is found that the narrow part of the channel requires a large pressure gradient, also in the narrow part the pressure gradient decreases with the increase in Weissenberg number *We* and channel width d.

Key words: Modeling of Hyperbolic Tangent Fluid Model; Asymmetric Channel; Analytical Solutions.

1. Introduction

Peristaltic transport is a well known process of a fluid transport which is induced by a progressive wave of area contraction or expansion along the length of distensible tube containing the fluid. It is used by many systems in the living body to propel or to mix the contents of a tube. The peristalsis mechanism usually occur in urine transport from kidney to bladder, swallowing food through the esophagus, chyme motion in the gastrointestinal tract, vasomotion of small blood vessels and movement of spermatozoa in the human reproductive tract. There are many engineering processes as well in which peristaltic pumps are used to handle a wide range of fluids particularly in chemical and pharmaceutical industries. It is also used in sanitary fluid transport, blood pumps in heart lung machine, and transport of corrosive fluids, where the contact of the fluid with the machinery parts is prohibited. Because most of the physiological fluids behave like a non-Newtonian fluid, therefore, some interesting studies dealing with the flows of non-Newtonian fluids are given in [1 – 15].

Motivated by possible applications in industry and physiology and previous studies regarding the peristaltic flows of Non-Newtonian fluid models, we discussed the tangent hyperbolic fluid model. The governing equations of hyperbolic tangent fluid model for peristaltic fluid flow in a two dimensional asymmetric channel has been modeled in the present paper. To the best of the authors knowledge no attempt has been made to study the hyperbolic tangent fluid model for peristaltic problems. The governing equations are reduced using long wave length approximation and then the reduced problem has been solved by the regular perturbation method. The expression for pressure rise is computed numerically using mathematics software Mathematica. At the end, the graphical results are presented to discuss the physical behaviour of various parameters of interest.

2. Fluid Model

For an incompressible fluid the balance of mass and momentum are given by

$$\mathrm{div}\boldsymbol{V} = 0, \tag{1}$$

$$\rho\frac{\mathrm{d}\boldsymbol{V}}{\mathrm{d}t} = \mathrm{div}\mathbf{S} + \rho\mathbf{f}, \tag{2}$$

where ρ is the density, $\boldsymbol{V}$ is the velocity vector, $\mathbf{S}$ is the Cauchy stress tensor, $\mathbf{f}$ represents the specific body force and $\mathrm{d}/\mathrm{d}t$ represents the material time derivative. The constitutive equation for hyperbolic tangent fluid is given by [10 – 11]

$$\mathbf{S} = -P\mathbf{I} + \boldsymbol{\tau}, \tag{3}$$

$$\boldsymbol{\tau} = -\left[\eta_\infty + (\eta_0 + \eta_\infty)\tanh(\Gamma\bar{\dot{\gamma}})^n\right]\bar{\dot{\gamma}}, \tag{4}$$

in which $-P\mathbf{I}$ is the spherical part of the stress due to constraint of incompressibility, $\boldsymbol{\tau}$ is the extra stress tensor, η_∞ is the infinite shear rate viscosity, η_0 is the zero shear rate viscosity, Γ is the time constant, n is the power law index, and $\bar{\dot{\gamma}}$ is defined as

$$\bar{\dot{\gamma}} = \sqrt{\frac{1}{2}\sum_i\sum_j \bar{\dot{\gamma}}_{ij}\bar{\dot{\gamma}}_{ji}} = \sqrt{\frac{1}{2}\boldsymbol{\Pi}}, \tag{5}$$

where $\boldsymbol{\Pi} = \frac{1}{2}\mathrm{trac}\left(\mathrm{grad}\boldsymbol{V} + (\mathrm{grad}\boldsymbol{V})^T\right)^2$.

Here $\boldsymbol{\Pi}$ is the second invariant strain tensor. We consider constitution (4), the case for which $\eta_\infty = 0$ and $\Gamma\bar{\dot{\gamma}} < 1$. The component of extra stress tensor, therefore, can be written as

$$\begin{aligned}\bar{\tau} &= -\eta_0[(\Gamma\bar{\dot{\gamma}})^n]\bar{\dot{\gamma}} = -\eta_0[(1+\Gamma\bar{\dot{\gamma}}-1)^n]\bar{\dot{\gamma}}\\ &= -\eta_0[1+n(\Gamma\bar{\dot{\gamma}}-1)]\bar{\dot{\gamma}}.\end{aligned} \tag{6}$$

3. Mathematical Formulation

Let us consider the peristaltic transport of an incompressible hyperbolic tangent fluid in a two dimensional channel of width $\bar{d}_1 + \bar{d}_2$. The flow is generated by sinusoidal wave trains propagating with constant speed c along the channel walls. The geometry of the wall surface is defined as

$$\begin{aligned}Y &= H_1 = \bar{d}_1 + \bar{a}_1\cos\left[\frac{2\pi}{\lambda}(\bar{X}-c\bar{t})\right],\\ Y &= H_2 = -\bar{d}_2 - \bar{b}_1\cos\left[\frac{2\pi}{\lambda}(\bar{X}-c\bar{t})+\phi\right],\end{aligned} \tag{7}$$

where $\bar{a}_1$ and $\bar{b}_1$ are the amplitudes of the waves, λ is the wave length, $\bar{d}_1+\bar{d}_2$ is the width of the channel, c is the velocity of propagation, $\bar{t}$ is the time, and $\bar{X}$ is the direction of wave propagation. The phase difference ϕ varies in the range $0 \le \phi \le \pi$ in which $\phi = 0$ corresponds to a symmetric channel with waves out of phase and $\phi = \pi$, the waves are in phase, further, $\bar{a}_1$, $\bar{b}_1$, $\bar{d}_1$, $\bar{d}_2$, and ϕ satisfies the condition

$$\bar{a}_1^2 + \bar{b}_1^2 + 2\bar{a}_1\bar{b}_1\cos\phi \le (\bar{d}_1+\bar{d}_2)^2.$$

The equations governing the flow of a tangent hyperbolic fluid are given by

$$\frac{\partial\bar{U}}{\partial\bar{X}} + \frac{\partial\bar{V}}{\partial\bar{Y}} = 0, \tag{8}$$

$$\rho\left(\frac{\partial\bar{U}}{\partial\bar{t}} + \bar{U}\frac{\partial\bar{U}}{\partial\bar{X}} + \bar{V}\frac{\partial\bar{U}}{\partial\bar{Y}}\right) = -\frac{\partial\bar{P}}{\partial\bar{X}} - \frac{\partial\bar{\tau}_{\bar{X}\bar{X}}}{\partial\bar{X}} - \frac{\partial\bar{\tau}_{\bar{X}\bar{Y}}}{\partial\bar{Y}}, \tag{9}$$

$$\rho\left(\frac{\partial\bar{V}}{\partial\bar{t}} + \bar{U}\frac{\partial\bar{V}}{\partial\bar{X}} + \bar{V}\frac{\partial\bar{V}}{\partial\bar{Y}}\right) = -\frac{\partial\bar{P}}{\partial\bar{Y}} - \frac{\partial\bar{\tau}_{\bar{X}\bar{Y}}}{\partial\bar{X}} - \frac{\partial\bar{\tau}_{\bar{Y}\bar{Y}}}{\partial\bar{Y}}. \tag{10}$$

We introduce a wave frame $(\bar{x},\bar{y})$ moving with velocity c away from the fixed frame $(\bar{X},\bar{Y})$ by the transformation

$$\begin{aligned}&\bar{x} = \bar{X} - c\bar{t}, \quad \bar{y} = \bar{Y}, \quad \bar{u} = \bar{U} - c,\\ &\bar{v} = \bar{V}, \ \text{and} \ \bar{p}(x) = \bar{P}(X,t).\end{aligned} \tag{11}$$

Further, we define

$$\begin{aligned}&x = \frac{\bar{x}}{\lambda}, \quad y = \frac{\bar{y}}{d_1}, \quad u = \frac{\bar{u}}{c}, \quad t = \frac{c}{\lambda}\bar{t},\\ &h_1 = \frac{\bar{h}_1}{\bar{d}_1}, \quad h_2 = \frac{\bar{h}_2}{\bar{d}_1}, \quad \tau_{xx} = \frac{\lambda}{\eta_0 c}\bar{\tau}_{\bar{x}\bar{x}},\\ &\tau_{xy} = \frac{\bar{d}_1}{\eta_0 c}\bar{\tau}_{\bar{x}\bar{y}}, \quad \tau_{yy} = \frac{\bar{d}_1}{\eta_0 c}\bar{\tau}_{\bar{y}\bar{y}}, \quad \delta = \frac{\bar{d}_1}{\lambda},\\ &\mathrm{Re} = \frac{\rho c\bar{d}_1}{\eta_0}, \quad We = \frac{\Gamma c}{d_1}, \quad P = \frac{\bar{d}_1^2}{c\lambda\eta_0}\bar{p},\\ &\dot{\gamma} = \frac{\bar{\dot{\gamma}}\bar{d}_1}{c}.\end{aligned} \tag{12}$$

Using the above non-dimensional quantities and the resulting equations in terms of stream function Ψ ($u = \frac{\partial\Psi}{\partial y}$, $v = -\delta\frac{\partial\Psi}{\partial x}$), (9) and (10) can be written as

$$\begin{aligned}&\delta\mathrm{Re}\left[\left(\frac{\partial\Psi}{\partial y}\frac{\partial}{\partial x} - \frac{\partial\Psi}{\partial x}\frac{\partial}{\partial y}\right)\frac{\partial\Psi}{\partial y}\right]\\ &= -\frac{\partial P}{\partial x} - \delta^2\frac{\partial\tau_{xx}}{\partial x} - \frac{\partial\tau_{xy}}{\partial y},\end{aligned} \tag{13}$$

$$\begin{aligned}&\delta^3\mathrm{Re}\left[\left(\frac{\partial\Psi}{\partial y}\frac{\partial}{\partial x} - \frac{\partial\Psi}{\partial x}\frac{\partial}{\partial y}\right)\frac{\partial\Psi}{\partial x}\right]\\ &= -\frac{\partial P}{\partial y} - \delta^2\frac{\partial\tau_{xy}}{\partial x} - \delta\frac{\partial\tau_{yy}}{\partial y},\end{aligned} \tag{14}$$

where

$$\tau_{xx} = -2[1+n(We\dot{\gamma}-1)]\frac{\partial^2\Psi}{\partial x\partial y},$$

$$\tau_{xy} = -[1+n(We\dot{\gamma}-1)]\left(\frac{\partial^2\Psi}{\partial y^2} - \delta^2\frac{\partial^2\Psi}{\partial x^2}\right),$$

$$\tau_{yy} = 2\delta[1+n(We\dot{\gamma}-1)]\frac{\partial^2\Psi}{\partial x\partial y},$$

$$\begin{aligned}\dot{\gamma} = \Bigg[&2\delta^2\left(\frac{\partial^2\Psi}{\partial x\partial y}\right)^2 + \left(\frac{\partial^2\Psi}{\partial y^2} - \delta^2\frac{\partial^2\Psi}{\partial x^2}\right)^2\\ &+ 2\delta^2\left(\frac{\partial^2\Psi}{\partial x\partial y}\right)^2\Bigg]^{1/2},\end{aligned}$$

in which δ, Re, We represent the wave, Reynolds, and Weissenberg numbers, respectively. Under the assumptions of long wavelength $\delta \ll 1$ and low Reynolds number, and neglecting the terms of order δ and higher, (13) and (14) take the form

$$\frac{\partial P}{\partial x} = \frac{\partial}{\partial y}\left[1+n\left(We\frac{\partial^2 \Psi}{\partial y^2}-1\right)\right]\frac{\partial^2 \Psi}{\partial y^2}, \quad (15)$$

$$\frac{\partial P}{\partial y} = 0. \quad (16)$$

Elimination of pressure from (15) and (16) yield

$$\frac{\partial^2}{\partial y^2}\left[1+n\left(We\frac{\partial^2 \Psi}{\partial y^2}-1\right)\right]\frac{\partial^2 \Psi}{\partial y^2} = 0. \quad (17)$$

The dimensionless mean flow Θ is defined by [2]

$$\Theta = F+1+d, \quad (18)$$

in which

$$F = \int_{h_2(x)}^{h_1(x)} \frac{\partial \Psi}{\partial y} dy = \Psi(h_1(x)) - \Psi(h_2(x)), \quad (19)$$

$$\begin{aligned} h_1(x) &= 1+a\cos 2\pi x, \\ h_2(x) &= -d-b\cos(2\pi x+\phi). \end{aligned} \quad (20)$$

The boundary conditions in terms of stream function Ψ are defined as:

$$\begin{aligned} \Psi &= \frac{F}{2}, \quad \frac{\partial \Psi}{\partial y} = -1 \text{ for } y = h_1(x), \\ \Psi &= -\frac{F}{2}, \quad \frac{\partial \Psi}{\partial y} = -1 \text{ for } y = h_2(x), \end{aligned} \quad (21)$$

where a, b, ϕ, and d satisfy the following relation:

$$a^2+b^2+2ab\cos\phi \le (1+d)^2.$$

4. Perturbation Solution

For the perturbation solution, we expand Ψ, F, and P as

$$\Psi = \Psi_0 + We\Psi_1 + O(We^2), \quad (22)$$

$$F = F_0 + WeF_1 + O(We^2), \quad (23)$$

$$P = P_0 + WeP_1 + O(We^2). \quad (24)$$

Substituting above expressions in (15), (17), and (21) and collecting the powers of We, we obtain the following systems:

4.1. System of Order We^0

$$\frac{\partial^4 \Psi_0}{\partial y^4} = 0, \quad (25)$$

$$\frac{\partial P_0}{\partial x} = (1-n)\frac{\partial^3 \Psi_0}{\partial y^3}, \quad (26)$$

$$\Psi_0 = \frac{F_0}{2}, \quad \frac{\partial \Psi_0}{\partial y} = -1 \text{ on } y = h_1(x), \quad (27)$$

$$\Psi_0 = -\frac{F_0}{2}, \quad \frac{\partial \Psi_0}{\partial y} = -1 \text{ on } y = h_2(x). \quad (28)$$

4.2. System of Order We^1

$$\frac{\partial^4 \Psi_1}{\partial y^4} = \frac{n}{n-1}\frac{\partial^2}{\partial y^2}\left(\frac{\partial^2 \Psi_0}{\partial y^2}\right)^2, \quad (29)$$

$$\frac{\partial P_1}{\partial x} = (1-n)\frac{\partial^3 \Psi_1}{\partial y^3} + n\frac{\partial}{\partial y}\left(\frac{\partial^2 \Psi_0}{\partial y^2}\right)^2, \quad (30)$$

$$\Psi_1 = \frac{F_1}{2}, \quad \frac{\partial \Psi_1}{\partial y} = 0 \text{ on } y = h_1(x), \quad (31)$$

$$\Psi_1 = -\frac{F_1}{2}, \quad \frac{\partial \Psi_1}{\partial y} = 0 \text{ on } y = h_2(x). \quad (32)$$

4.3. Solution for System of Order We^0

Solution of (25) satisfying the boundary conditions (27) and (28) can be written as:

$$\begin{aligned} \Psi_0 = {} & \frac{F_0+h_1-h_2}{(h_2-h_1)^3}(2y^3-3(h_1+h_2)y^2+6h_1h_2y) \\ & -y+\frac{1}{(h_2-h_1)^3}\left[\left(\frac{F_0}{2}+h_1\right)(h_2^3-3h_1h_2^2) \right. \\ & \left. -\left(h_2-\frac{F_0}{2}\right)(h_1^3-3h_2h_1^2)\right]. \end{aligned} \quad (33)$$

The axial pressure gradient at this order is

$$\frac{\mathrm{d}P_0}{\mathrm{d}x} = \frac{12(1-n)(F_0+h_1-h_2)}{(h_2-h_1)^3}. \quad (34)$$

For one wavelength the integration of (34) yields

$$\Delta P_{\lambda_0} = \int_0^1 \frac{\mathrm{d}P_0}{\mathrm{d}x}\mathrm{d}x. \quad (35)$$

4.4. Solution for System of Order We^1

Substituting the zeroth-order solution (33) into (29), the solution of the resulting problem satisfying the boundary conditions take the following form:

$$\Psi_1 = C_0 + C_1 y + C_2\frac{y^2}{2!} + C_3\frac{y^3}{3!} + \frac{288n}{n-1}\left[\frac{F_0+h_1-h_2}{(h_2-h_1)^3}\right]^2\frac{y^4}{4!}, \tag{36}$$

where

$$C_0 = -\frac{6}{(h_2-h_1)^3}\left[F_1 - \frac{A}{4!}(h_1^3(2h_2-h_1) - h_2^3(2h_1-h_2))\right]\left[\frac{h_1h_2^2}{2}-\frac{h_2^3}{6}\right] - \frac{A}{3!}\left(\frac{h_1^2h_2^2}{2}+\frac{h_1h_2^3}{2}-\frac{h_2^4}{4}\right) - \frac{F_1}{2},$$

$$C_1 = \frac{6h_1h_2F_1}{(h_2-h_1)^3} + \frac{Ah_1h_2}{2}\left[\frac{(h_1+h_2)}{3} - \frac{1}{2(h_2-h_1)^3}\cdot\Big(h_1^3(2h_2-h_1)-h_2^3(2h_1-h_2)\Big)\right],$$

$$C_2 = \frac{-6F_1(h_1+h_2)}{(h_2-h_1)^3} + A\left[\frac{(h_1+h_2)}{4(h_2-h_1)^3}\Big(h_1^3(2h_2-h_1) - h_2^3(2h_1-h_2)\Big) - \frac{h_1^2+h_1h_2+h_2^2}{3!}\right],$$

$$C_3 = \frac{12}{(h_2-h_1)^3}\left[F_1 - \frac{A}{4!}\Big(h_1^3(2h_2-h_1) - h_2^3(2h_1-h_2)\Big)\right],$$

$$A = \frac{n}{n-1}288\left[\frac{F_0+h_1-h_2}{(h_2-h_1)^3}\right]^2.$$

The axial pressure gradient at this order is

$$\frac{\mathrm{d}P_1}{\mathrm{d}x} = (1-n)C_3 - 144n(h_1+h_2)\left[\frac{F_0+h_1-h_2}{(h_2-h_1)^3}\right]^2. \tag{37}$$

For one wavelength the integration of (37) yields

$$\Delta P_{\lambda_1} = \int_0^1 \frac{\mathrm{d}P_1}{\mathrm{d}x}\mathrm{d}x. \tag{38}$$

Summarizing the perturbation results for small parameter We, the expression for stream functions and pressure gradient can be written as:

$$\begin{aligned}\Psi = {}& \frac{F+h_1-h_2}{(h_2-h_1)^3}\Big(2y^3 - 3(h_1+h_2)y^2 + 6h_1h_2y\Big) \\ &- y + \frac{1}{(h_2-h_1)^3}\left[\left(\frac{F}{2}+h_1\right)(h_2^3-3h_1h_2^2) - \left(h_2-\frac{F}{2}\right)(h_1^3-3h_2h_1^2)\right] \\ &+ We\left[B + Cy + D\frac{y^2}{2!} + E\frac{y^3}{3!} + A_1\frac{y^4}{4!}\right],\end{aligned} \tag{39}$$

$$\begin{aligned}\frac{\mathrm{d}P}{\mathrm{d}x} = {}& \frac{12(1-n)(F+h_1-h_2)}{(h_2-h_1)^3} \\ &+ We\left[-\frac{12(1-n)}{(h_2-h_1)^3}\frac{A_1}{4!}\Big(h_1^3(2h_2-h_1) - h_2^3(2h_1-h_2)\Big) - 144n(h_1+h_2)\left(\frac{F+h_1-h_2}{(h_2-h_1)^3}\right)^2\right],\end{aligned} \tag{40}$$

where

$$B = -\frac{6}{(h_2-h_1)^3}\left[\frac{A_1}{4!}\Big(h_1^3(2h_2-h_1) - h_2^3(2h_1-h_2)\Big)\right]\cdot\left(\frac{h_1h_2^2}{2}-\frac{h_2^3}{6}\right) - \frac{A_1}{3!}\left(\frac{h_1^2h_2^2}{2}+\frac{h_1h_2^3}{2}-\frac{h_2^4}{4}\right),$$

$$C = \frac{A_1h_1h_2}{2}\left[\frac{(h_1+h_2)}{3} - \frac{1}{2(h_2-h_1)^3}\Big(h_1^3(2h_2-h_1) - h_2^3(2h_1-h_2)\Big)\right],$$

$$D = A_1\left[\frac{(h_1+h_2)}{4(h_2-h_1)^3}\Big(h_1^3(2h_2-h_1) - h_2^3(2h_1-h_2)\Big) - \frac{(h_1^2+h_1h_2+h_2^2)}{3!}\right],$$

$$E = \frac{12}{(h_2-h_1)^3}\left[\frac{A_1}{4!}\Big(h_1^3(2h_2-h_1) - h_2^3(2h_1-h_2)\Big)\right],$$

$$A_1 = \frac{n}{n-1}288\left[\frac{F+h_1-h_2}{(h_2-h_1)^3}\right]^2.$$

In the above solution when $\dot{\gamma} \longrightarrow 0$ then $\mu \longrightarrow \mu_0$, (or $n=0$) the solutions of Mishra and Rao [16] are a special case of our problem.

The non-dimensional pressure rise over one wavelength ΔP_λ for the axial velocity are

$$\Delta P_\lambda = \int_0^1 \frac{\mathrm{d}P}{\mathrm{d}x}\mathrm{d}x, \tag{41}$$

where $\mathrm{d}P/\mathrm{d}x$ is defined in (40).

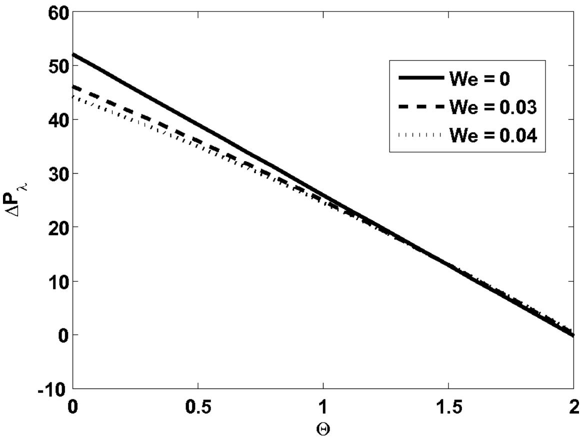

Fig. 1. Variation of ΔP_λ with Θ for different values of We at $a = 0.5$, $b = 0.5$, $d = 0.4$, $n = 0.04$, and $\phi = \frac{\pi}{6}$.

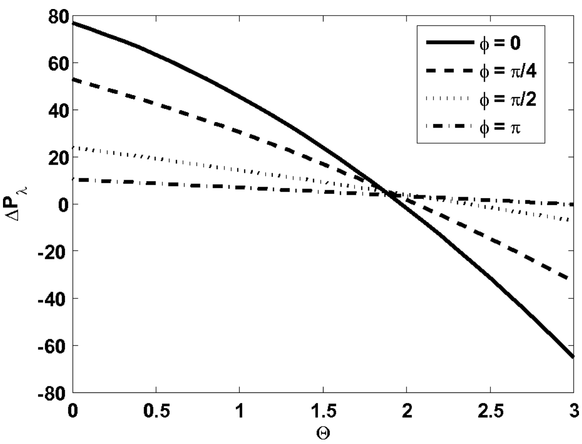

Fig. 2. Variation of ΔP_λ with Θ for different values of ϕ at $a = 0.5$, $d = 0.5$, $We = 0.03$, $n = 0.04$, and $b = 0.7$.

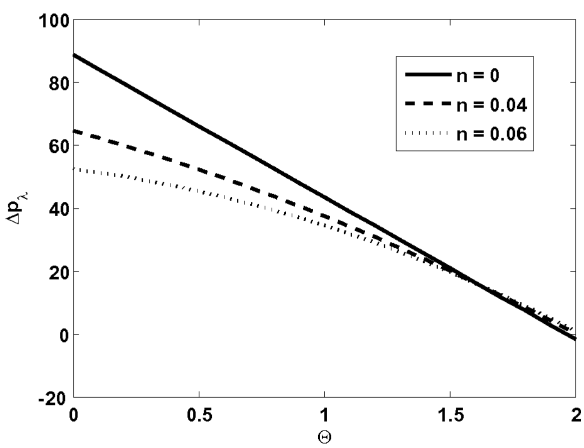

Fig. 3. Variation of ΔP_λ with Θ for different values of n at $a = 0.5$, $d = 0.5$, $We = 0.03$, $b = 0.7$, and $\phi = \frac{\pi}{6}$.

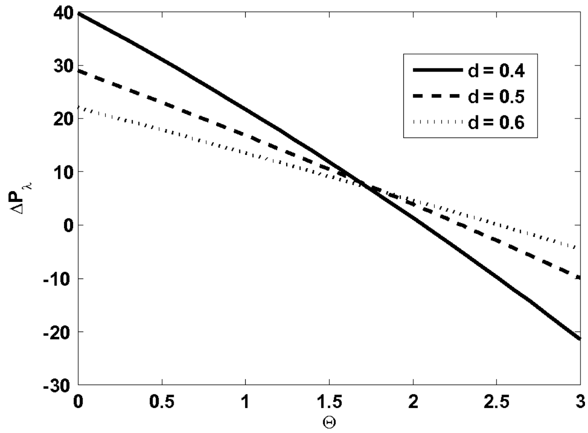

Fig. 4. Variation of ΔP_λ with Θ for different values of d at $a = 0.5$, $b = 0.5$, $We = 0.03$, $n = 0.04$, and $\phi = \frac{\pi}{4}$.

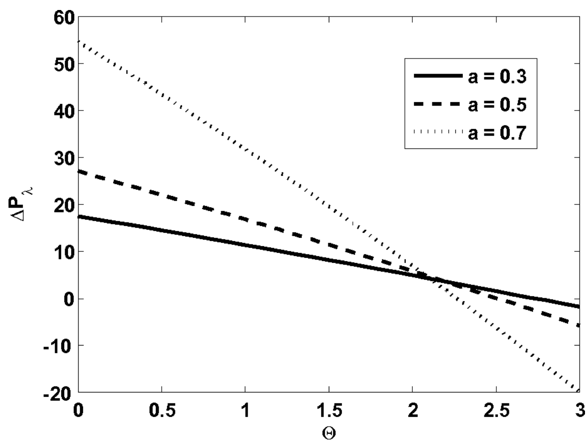

Fig. 5. Variation of ΔP_λ with Θ for different values of a at $b = 0.7$, $d = 0.7$, $We = 0.03$, $n = 0.04$, and $\phi = \frac{\pi}{4}$.

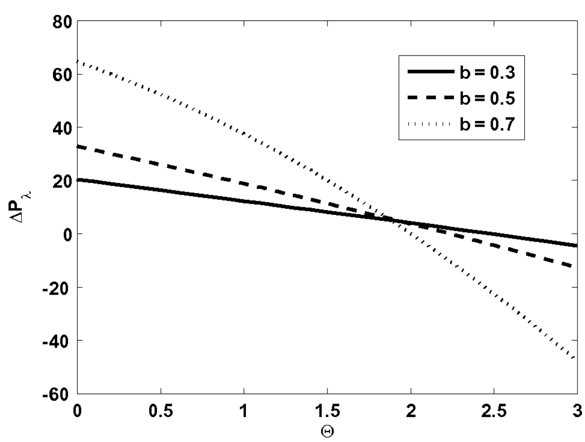

Fig. 6. Variation of ΔP_λ with Θ for different values of b at $a = 0.5$, $d = 0.5$, $We = 0.03$, $n = 0.04$, and $\phi = \frac{\pi}{6}$.

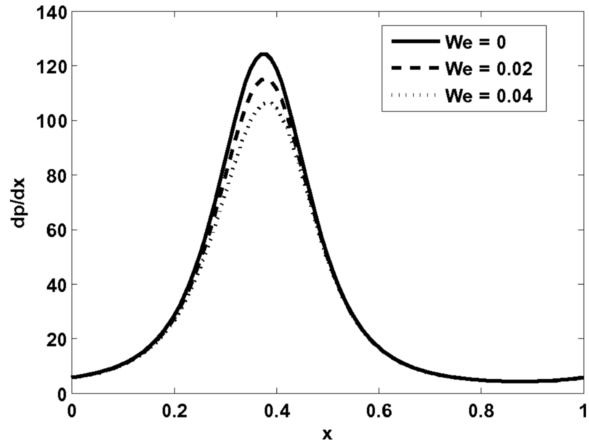

Fig. 7. Variation of $\frac{\mathrm{d}p}{\mathrm{d}x}$ with x for different values of We at $a = 0.5$, $b = 0.5$, $d = 0.2$, $n = 0.04$, $\Theta = 0.4$, and $\phi = \frac{\pi}{2}$.

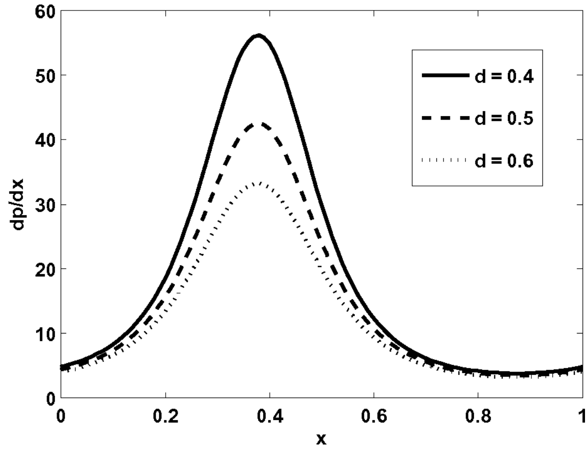

Fig. 8. Variation of $\frac{\mathrm{d}p}{\mathrm{d}x}$ with x for different values of d at $a = 0.5$, $b = 0.5$, $We = 0.03$, $n = 0.04$, $\Theta = 0.4$, and $\phi = \frac{\pi}{2}$.

(a)

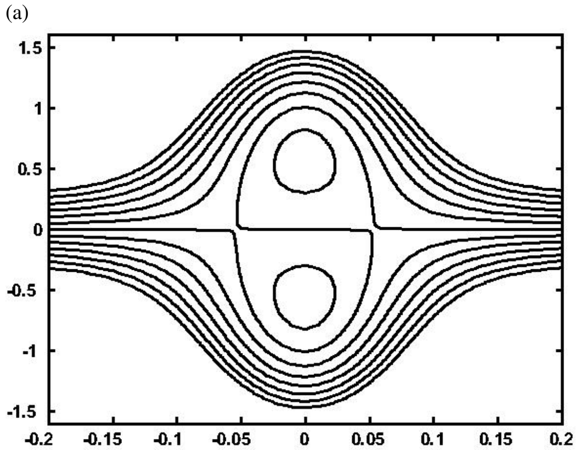

(b)

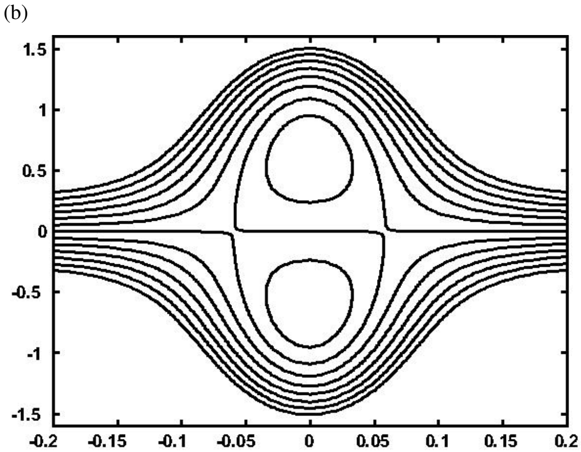

(c)

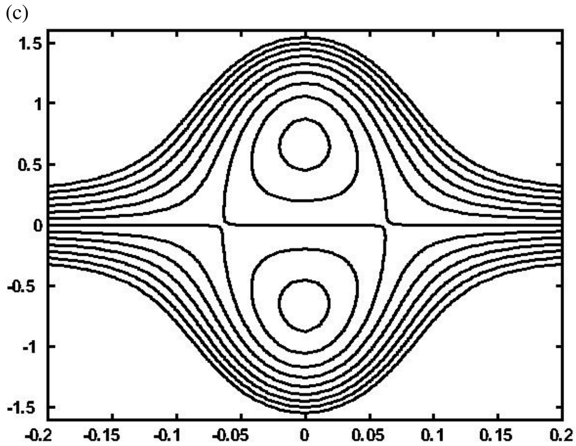

Fig. 9. Stream lines for three different values of Q. (a) for $Q = 0.24$, (b) for $Q = 0.25$, (c) for $Q = 0.26$. The other parameters are chosen as $a = 0.5$, $b = 0.5$, $d = 1.0$, $n = 0.09$, $We = 0.04$, and $\phi = 0.01$.

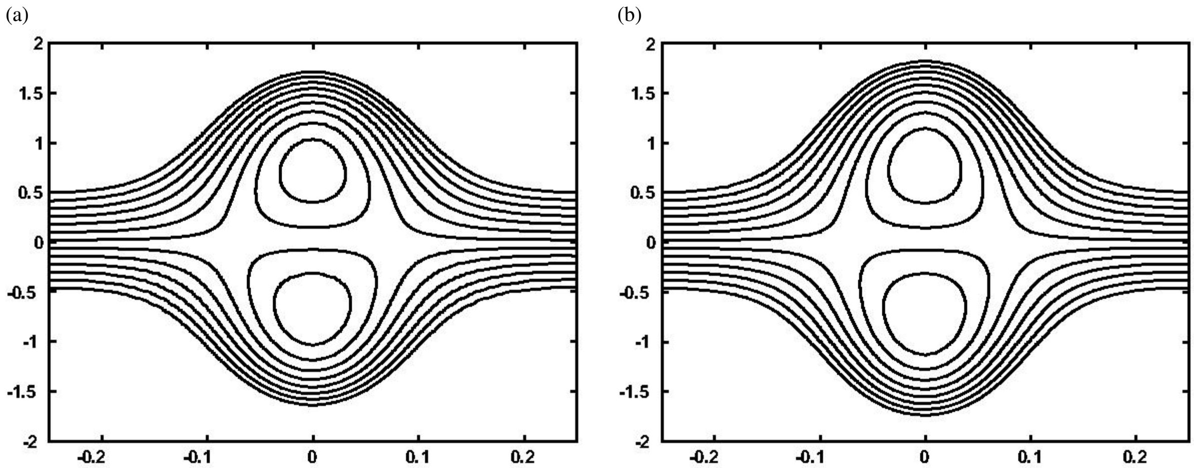

Fig. 10. Stream lines for two different values of We. (a) for $We = 0.4$, (b) for $We = 0.04$. The other parameter are chosen as $a = 0.54$, $b = 0.5$, $d = 1.0$, $n = 0.09$, $Q = 0.25$, and $\phi = 0.01$.

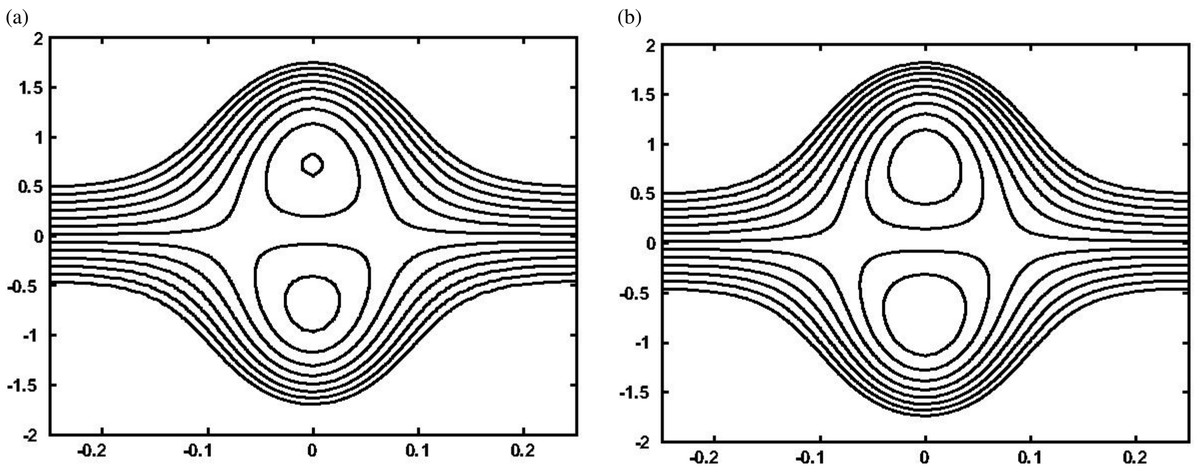

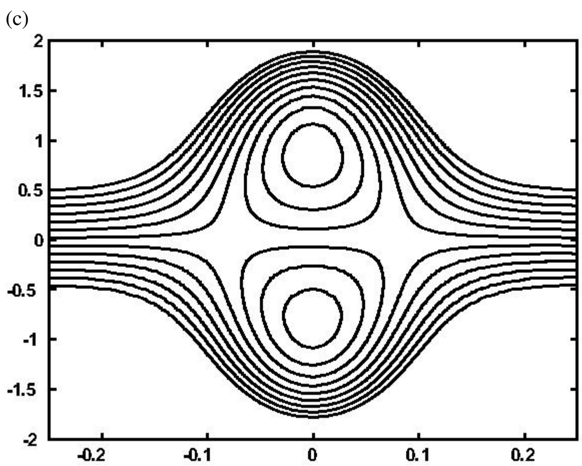

Fig. 11. Stream lines for three different values of a. (a) for $a = 0.52$, (b) for $a = 0.54$, (c) for $a = 0.56$. The other parameters are chosen as $b = 0.5$, $d = 1.0$, $Q = 0.3$, $\phi = 0.01$, $We = 0.04$, and $n = 0.09$.

5. Results and Discussion

The analytical solution of the hyperbolic tangent model is presented. The expression for pressure rise ΔP_λ is calculated numerically using mathematics software. The effects of various parameters on the pressure rise ΔP_λ are shown in Figures 1 – 6 for various values of Weissenberg number We, amplitude ratio ϕ, tangent hyperbolic power law index n, channel width d, and wave amplitudes a, b. It is observed from Figure 1 that pressure rise decreases for small values of Θ ($0 \le \Theta \le 1.45$) with the increase in We and for large Θ ($1.45 \le \Theta \le 2$), the pressure rise increases. We also observe that for different values of We, there is a linear relation between ΔP_λ and Θ, i. e., the pressure rise decreases for small Θ and increases for large Θ. The pressure rise ΔP_λ for different values of ϕ are illustrated in Figure 2. It is shown that ΔP_λ decreases with the increase in ϕ for $\Theta \in [0, 1.9]$ and after that ΔP_λ increases. The graphs of ΔP_λ for different values of power law index n are presented in Figure 3. It is seen that with the increase in n, ΔP_λ decreases for $\Theta \in [0, 1.6]$ and for $\Theta \in [1.6, 2]$ it is increasing. It is observed that the pressure rise decreases with the increase in d and increases with the increase in a and b for small Θ and for large Θ, the results are opposite (see Figs. 4 – 6). Figures 7 and 8 represent that for $x \in [0, 0.2]$ and $[0.6, 1]$ the pressure gradient is small, we say that the flow can easily pass without imposition of large pressure gradient, while in the narrow part of the channel $x \in [0.2, 0.6]$, to retain same flux, large pressure gradient is required. Moreover in the narrow part of the channel, the pressure gradient decreases with the increase in We and d.

5.1. Trapping Phenomena

Another interesting phenomena in peristaltic motion is trapping. It is basically the formation of an internally circulating bolus of fluid by closed stream lines. This trapped bolus pushed a head along peristaltic waves. Figures 9 – 11 illustrate the stream lines for different values of Q, We, and a. The stream lines for different values of volume flow rate Q are shown in Figure 9. It is found that with the increase in volume flow rate Q, the size and the number of trapping bolus increases. In Figure 10 the stream lines are prepared for different value of Weissenberg number We. It is depicted that the size of the trapped bolus increases with the increase in We. It is observed from Figure 11 that the size and the number of the trapping bolus increases with the increases in amplitude of the wave a.

6. Conclusion

In the present paper we have investigated the peristaltic flow of tangent hyperbolic fluid in an asymmetric channel. The governing two dimensional equations have been modeled and then simplified using long wave length approximation. The simplified equations are solved analytically using regular perturbation method. The results are discussed through graphs. We conclude the following observations:

1. It is observed that in the peristaltic pumping region the pressure rise decreases with the increases in We, ϕ, n, and d, and increases with the increases in a and b.
2. The pressure gradient decreases with the increases in both We and d.
3. The size of the trapping bolus increases with the increases in Q, We and decreases with the increases in a.

[1] T. Hayat, F.M. Mahomed, and S. Asghar, Nonlinear Dynamics **40**, 375 (2005).

[2] T. Hayat and N. Ali, Appl. Math. Computation **193**, 535 (2007).

[3] D. Srinivasacharya, M. Mishra, and A.R. Rao, Acta Mechanica **161**, 165 (2003).

[4] T. Hayat, Y. Wang, A.M. Siddiqui, and K. Hutter, Math. Probl. Eng. **1**, 1 (2003).

[5] T. Hayat and N. Ali, Physica A **371**, 188 (2006).

[6] M. Ealshahed and M.H. Haroun, Probl. Eng. **6**, 663 (2005).

[7] T. Hayat, N. Ahmad, and N. Ali, Commun. Nonlinear Science and Numerical Simulation **13**, 1581 (2008).

[8] M.H. Haroun, Computation Material Science **39**, 324 (2007).

[9] T. Hayat and N. Ali, Physica A **370**, 225 (2006).

[10] T. Hayat, N. Ali, and Z. Abbas, Phys. Lett. A **370**, 331 (200).

[11] L. Ai and K. Vafai, Numer. Heat Transfer, part A, **47**, 955 (2005).

[12] I. Pop and D.B. Ingham, Convective heat transfer: Mathematical and computational modeling of viscous

fluids and porous media, Pergamon, Amsterdam, New York 2001.

[13] A. H. Shapiro, M. Y. Jaffrin, and S. L. Weinberg, J. Fluid Mech. **37**, 799 (1969).

[14] M. H. Haroun, Commun. Nonlin. Sci. Numer. Simul. **12**, 1464 (2007).

[15] Y. Wang, T. Hayat, and K. Hutter, Intern. J. Nonlinear Mech. **40**, 40 (2005).

[16] M. Mishra and A. R. Rao, Z. angew. Math. Phys. **54**, 532 (2004).